

Density Functional Theory-Based Database Development and CALPHAD Automation

YI WANG,^{1,2} SHUNLI SHANG,^{1,3} LONG-QING CHEN,^{1,4} and ZI-KUI LIU^{1,5}

1.—Department of Materials Science and Engineering, The Pennsylvania State University, University Park, PA 16802-5006, USA. 2.—e-mail: yuw3@psu.edu. 3.—e-mail: sus26@psu.edu. 4.—e-mail: lqc3@psu.edu. 5.—e-mail: zxl15@psu.edu

We report our research activities on density functional theory-based alloy thermodynamics, including method/software developments, the integration of first-principles calculations, CALPHAD modeling, and the automation of phase diagram calculations. Examples to be discussed include phonon dispersions of rhombohedral BiFeO_3 , the solution to the long-outstanding problem of imaginary phonon frequencies for cubic perovskites using EuTiO_3 as an example, the calculation of excess specific heat for the magnetic phase transition in EuTiO_3 , and the automated calculation of a phase diagram for the Al-Mg system.

INTRODUCTION

In thermodynamics, a phase is defined as a region in the configurational space throughout which the desired physical properties of a material are essentially uniform, dictated by the conditions of temperature, pressure, and chemical composition. In other words, the properties of a multicomponent material, such as structure, density, electric, magnetic, mechanical, and thermodynamic properties, *etc.*, are uniquely decided by its state or phase. Accordingly, one of the central tasks in the community of the material sciences is the accurate description of the phase diagram manifested by the relative stabilities of a variety of phases as functions of temperature and composition. For this purpose, computational thermodynamics, based on the CALPHAD (calculation of phase diagram) approach¹ developed in the last few decades, has released the power of thermodynamics and enabled scientists and engineers to make phase stability calculations routinely by the support of increasingly available experimental data compensated by the first-principles calculation.

A specific CALPHAD model usually follows the following sequences: collecting the thermochemical and phase boundary data and then making the appropriate thermodynamic model, followed by the evaluation of modeling parameters of individual phases and then refining the parameters for the best description of the phase boundaries. Finally,

the modeling parameters are collected in databases, covering the whole composition and temperature ranges, including experimentally uninvestigated regions, establishing the foundation for a broad collaboration in developing multicomponent thermodynamic databases. However, the thermochemical and phase boundary data, either from experiments or theoretical calculations, are often scattered in the literature, requiring a significant amount of work to collect and analyze them. Moreover, these data are usually not kept electronically after the thermodynamic modeling is completed, which is not only a loss of valuable data but also makes the revision of multicomponent thermodynamic databases an extremely daunting task.

Due to the advances in both computer power and the efficiency of computational methods in the past few years, the first-principles quantum mechanics technique based on density functional theory has made significant progresses and demonstrated in many cases the accuracy of predicted thermodynamic properties comparable with experimental uncertainties.²⁻⁹ This progress implies that the first-principles calculations have enabled the CALPHAD modeling available even for a system with little experimental data. Currently, the data that can be provided by first-principles calculation typically include: (I) the enthalpy of formation, the relative lattice stability, and the defect structure and lattice preference at 0 K; (II) thermodynamics at finite temperatures by phonon or Debye approach; (III)

enthalpy of mixing in binary and ternary substitutional solutions or random phases based on the selected quasi-random structures; and (IV) structure of liquid, super-cooled liquid, and glass by means of *ab initio* molecular dynamics simulations.

The aim of this article is to give a summary of our research works on density functional theory-based alloy thermodynamics. The rest of this article is sectioned as follows: After an introduction to the computational scheme of the CALPHAD approach (“[The CALPHAD Approach](#)” section), we brief the first-principles phonon theory on thermodynamics for single configuration phase (“[First-Principles Theory of Thermodynamics for Phase with Single Microstate](#)” section). We then give a summary of the mixed-space approach to the phonons of polar materials (“[Mixed-Space Approach for Phonons of Polar Materials](#)” section), which is followed by introducing the YPHON package—the computerization of the mixed-space approach (“[YPHON Package](#)” section); continually is our first-principles solution to phase with thermal mixture among multiple micromagnetic states (“[First-Principles Theory of Thermodynamics for Phase with Thermal Mixture Among Multiple Micromagnetic States](#)” section). After that is a summary of our work on automating phase diagram calculation—ESPEI modeling automation (“[ESPEI Modeling Automation](#)” section). Finally, the last section concludes the paper.

THE CALPHAD APPROACH

The calculation of phase diagram at least requires the information of the Gibbs free energies of all possible phases as functions of both temperature and chemical compositions, no matter whether the phases are stable (lowest Gibbs free energy among all phases) or metastable, or even not measurable at a specific temperature. By formulation, the general form of the Gibbs free energy for a phase α in the CALPHAD approach is written as

$$G^\alpha = {}^0G^\alpha + \Delta G^\alpha \quad (1)$$

where G^α is the Gibbs free energy of the multicomponent α phase, ${}^0G^\alpha$ represents the mechanical mixing of individual species, and ΔG^α denotes the interactions among the species or endmembers. ${}^0G^\alpha$ and ΔG^α are commonly written as follows:

$${}^0G^\alpha = \sum x_i {}^0G_i^\alpha \quad (2)$$

$$\begin{aligned} \Delta G^\alpha = & \Delta G_{\text{conf}}^\alpha + \sum_i \sum_{j>i} x_i x_j \sum_{n=0}^n L_{ij}^\alpha (x_i - x_j)^n \\ & + \sum_i \sum_{j>i} \sum_{k>j} x_i x_j x_k L_{ijk}^\alpha \end{aligned} \quad (3)$$

where x_i is the mole fraction of species i , ${}^0G_i^\alpha$ is the Gibbs free energy of species i in the structure of the α phase, $\Delta G_{\text{conf}}^\alpha$ the configurational contribution,

and ${}^nL_{i,j}^\alpha$ and L_{ijk}^α are binary and ternary interaction parameters and can be temperature dependent. For most thermodynamic modelings, $\Delta G_{\text{conf}}^\alpha$ is usually assumed to be from the ideal atomic configurational entropy of mixing as

$$-T\Delta S_{\text{conf}} = RT \sum x_i \ln x_i. \quad (4)$$

The CALPHAD approach was then transformed into the modeling and the evaluation of the interaction parameters ${}^nL_{i,j}^\alpha$ and L_{ijk}^α in Eq. 3 aimed at the best description of the experimental phase boundaries as well as the experimental phase equilibrium and thermochemical data. For pure elements and stoichiometric compounds, the most commonly used model is the one suggested by the Scientific Group Thermodata Europe (SGTE). The CALPHAD approach has been extended to model multi-component atomic mobility, molar volume, and elastic coefficients¹⁰ for which the configurational contribution in Eq. 4 can be neglected.

Generally speaking, the types of phases should be considered in a CALPHAD modeling are as follows:

1. Pure elements in different crystal structures
2. Stoichiometric compounds
3. Solution phases typically with the matrix structures of face-centered cubic (fcc), body-centered cubic (bcc), hexagonal close packed (hcp), and various compounds with homogeneity ranges
4. Amorphous and liquid phases
5. Gas phases

Most input data to the CALPHAD modeling can be in principle obtained by first-principles calculations. For instance, the formation enthalpies are not strongly dependent on the temperature. Therefore, for pure elements in different crystal structures and stoichiometric compounds, inputs related to formation enthalpies to Eq. 3 can be approximated by the first-principles 0 K formation energies.² Regarding the solution phases or random phases, an efficient approximation to calculate the enthalpies of mixing is using the special quasi-random structures.^{6,11} For amorphous, glass, or liquid phases, the *ab initio* molecular dynamical simulation can be a compensating choice.¹²

FIRST-PRINCIPLES THEORY OF THERMODYNAMICS FOR PHASE WITH SINGLE MICROSTATE

Within the framework of single phase theory, at given atomic volume V and temperature T , the Helmholtz free energy is written as follows^{3,7}:

$$F(V, T; \sigma) = E_c(V; \sigma) + F_{\text{vib}}(V, T; \sigma) + F_{\text{el}}(V, T; \sigma) \quad (5)$$

where E_c , F_{vib} , and F_{el} represent the 0 K static energy, the vibrational contribution to the free energy, and the thermal electronic contribution to the free energy, respectively. The symbol σ in Eq. 5 is used

to label the microstate. In particular, F_{vib} is related to the phonon density of states (PDOS) by

$$F_{\text{vib}}(V, T; \sigma) = k_{\text{B}}T \int \ln \left\{ 2 \sinh \left[\frac{\hbar\omega}{2k_{\text{B}}T} \right] \right\} \text{PDOS}(\omega) d\omega \quad (6)$$

where ω represents phonon frequency. Currently, most first-principles methods in calculating the phonon frequencies are limited by the supercell size or the number exact wave vector points. That is, the dynamical matrices used to evaluate the phonon frequency are not explicitly known everywhere in the Brillouin zone. For computational reasons, they are only obtained for a small set of wave vectors. A $4 \times 4 \times 4$ supercell cell built on the primitive unit cell or $4 \times 4 \times 4$ exact wave vector mesh is usually the common limit. In this case, a numerical interpolation technique is required to obtain the phonon frequencies for more condensed wave vector meshes. For that purpose, the use of a discrete Fourier transform is one of the best choices.

MIXED-SPACE APPROACH FOR PHONONS OF POLAR MATERIALS

Currently, there are essentially two methods in use for the first-principles calculations of phonon frequencies: the linear response theory and the direct approach. The linear response theory directly evaluates the dynamical matrix through the density functional perturbation theory. In comparison, the advantage of mixed-space approach over the often used linear-response method is that it can be applied with the use of any code capable of computing forces. The direct approach is also referred to as the small displacement approach, the supercell method, or the frozen phonon approach.

However, most of the previous implementations of the supercell approach cannot accurately handle the long range dipole–dipole interactions when calculating phonon properties of a polar material. Our mixed-space approach^{4,9} has resolved this long-standing problem. By explicitly taking into account the effects of vibration-induced dipole–dipole interactions between periodic supercells, the mixed-space approach has made it possible to determine accurately the lattice dynamics of polar materials within the direct approach.

By the mixed-space approach,^{4,9} the dynamical matrix for an arbitrary wave vector \mathbf{q} is written as

$$D_{\alpha\beta}^{jk}(\mathbf{q}) = \frac{1}{\sqrt{\mu_j \mu_k}} \sum_P^{N_c} \left[\varphi_{\alpha\beta}^{jk}(P, 0) + \frac{d_{\alpha\beta}^{jk}(na)}{N_c} \right] \times \exp\{i\mathbf{q} \cdot [\mathbf{R}(P) + \mathbf{r}(j) - \mathbf{R}(0) - \mathbf{r}(k)]\} \quad (7)$$

where μ_j represents the atomic mass of the atom at the j th lattice site of the primitive unit cell, N_c is the number of primitive unit cell in the supercell,

$\varphi_{\alpha\beta}^{jk}(P, 0)$ represents the cumulative force constants that are usually the direct output of most first-principles codes, and

$$d_{\alpha\beta}^{jk}(na) = \frac{4\pi e^2}{V_a} \frac{[\mathbf{q} \cdot \mathbf{Z}^*(j)]_{\alpha} [\mathbf{q} \cdot \mathbf{Z}^*(k)]_{\beta}}{\mathbf{q} \cdot \boldsymbol{\varepsilon}_{\infty} \cdot \mathbf{q}} \Big|_{\mathbf{q} \rightarrow 0} \quad (8)$$

where $\mathbf{Z}^*(j)$ represents the Born effective charge tensor of the j th atom in the primitive unit cell, and $\boldsymbol{\varepsilon}_{\infty}$ is the high frequency static dielectric tensor, i.e., the contribution to the dielectric permittivity tensor from the electronic polarization.

The mixed approach has been demonstrated within our group^{10,13–17} and outside our group^{18,19} for a variety of materials.

YPHON PACKAGE

YPHON represents a package, written mainly in C++ code, implementing the mixed-space approach within the direct approach. YPHON makes full use of the accuracy of the force constants calculated in the real space and the dipole–dipole interactions in the reciprocal space, making the accurate phonon calculation possible with the direct method for polar materials besides the linear response method. After 3 years of extensive tests, we are now working to distribute the YPHON package as open source. The Microsoft Windows (Microsoft Corporation, Redmond, WA) graphical user interface (GUI) of YPHON is illustrated in Fig. 1.

The functions in the current YPHON package include the following:

1. The calculation of the phonon dispersions
2. The calculation of the PDOS
3. The calculation of the neutron scattering section weighted PDOS
4. The dynamic short range fluctuation approach to the system with static phonon instability (imaginary modes)
5. The calculation of the phonon dispersions for random alloys
6. The symmetry analysis of the vibrational modes using the point group theory

Figure 2 demonstrates the application YPHON to bismuth ferrite (BiFeO_3), which is an extensively studied room-temperature multiferroic material. At the time when the calculated phonon dispersions of BiFeO_3 were published,¹⁷ no experimental data for both PDOS and phonon dispersions were available. The calculated PDOS of BiFeO_3 was verified later by the inelastic neutron scattering experiment by Delaire et al.²⁰ Very recently, Borissenko et al.²¹ reported an inelastic x-ray scattering measurement for the phonon dispersions of BiFeO_3 . Our replotted phonon dispersions based on our previous calculations¹⁷ show excellent agreement with the inelastic x-ray scattering measurement.²¹

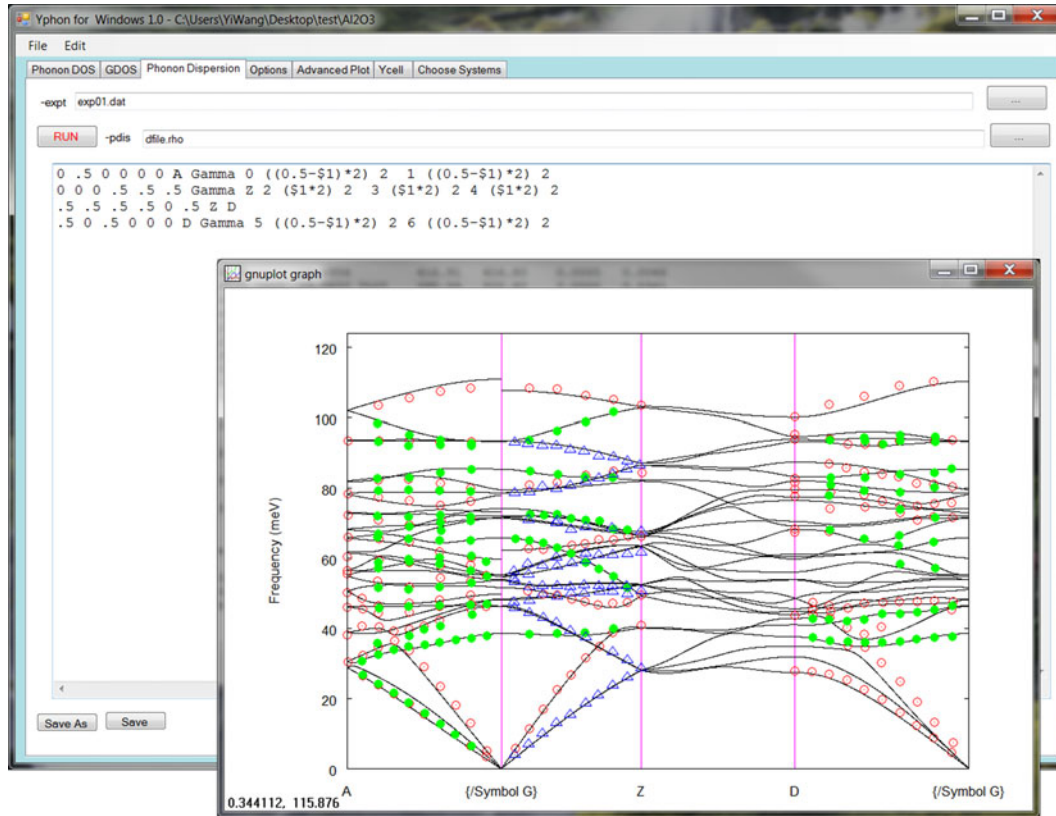


Fig. 1. GUI for the YPHON package exemplified with the calculation of the phonon dispersions for Al_2O_3 (Color figure online).

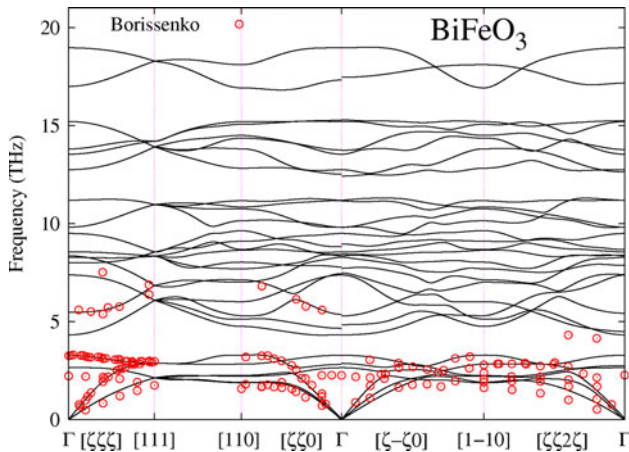


Fig. 2. The calculated phonon dispersions (curves) for rhombohedral BiFeO_3 with the mixed-space approach in comparison with inelastic x-ray scattering data²¹ (points) (Color figure online).

Figure 3^{22,23} is a preliminary demonstration of our ongoing work using a dynamic short range ordering model within YPHON for the calculation of phonon dispersions of cubic europium titanate (EuTiO_3) compared with those calculated with the conventional static displacive model.²⁴ We can declare that for EuTiO_3 , we have solved two long-existing problems. The first problem is that in the

community it has been thought for many decades that the direct method cannot be employed to accurately calculate the phonon properties of a polar material as showed by the calculated phonon dispersions of a variety of structures of EuTiO_3 by Rushchanskii et al.²⁴ The most recent demonstration of the mixed space approach and YPHON is for CaF_2 and CeO_2 ,²⁵ by which we have resolved the existing disagreements between experimental measurements and previous calculations using the Vienna ab initio simulation package (VASP), plane-wave self-consistent field (PWSCF), and ABINIT in the literature.

With EuTiO_3 , the second problem is concerned with the imaginary phonon frequency, typically existed for most Perovskites when calculation is performed based on the static cubic structure, which has been blocking the application of the phonon approach for the accurate calculation of thermodynamic properties. Compared with the calculated phonon dispersions shown in Fig. 3b using the conventional static displacive model, which results in imaginary phonon frequencies (shown as negative number) around the M and R points, we see that the imaginary phonon frequency problem disappeared in Fig. 3a by our dynamic short-range ordering model implemented in YPHON (the details will be published elsewhere).

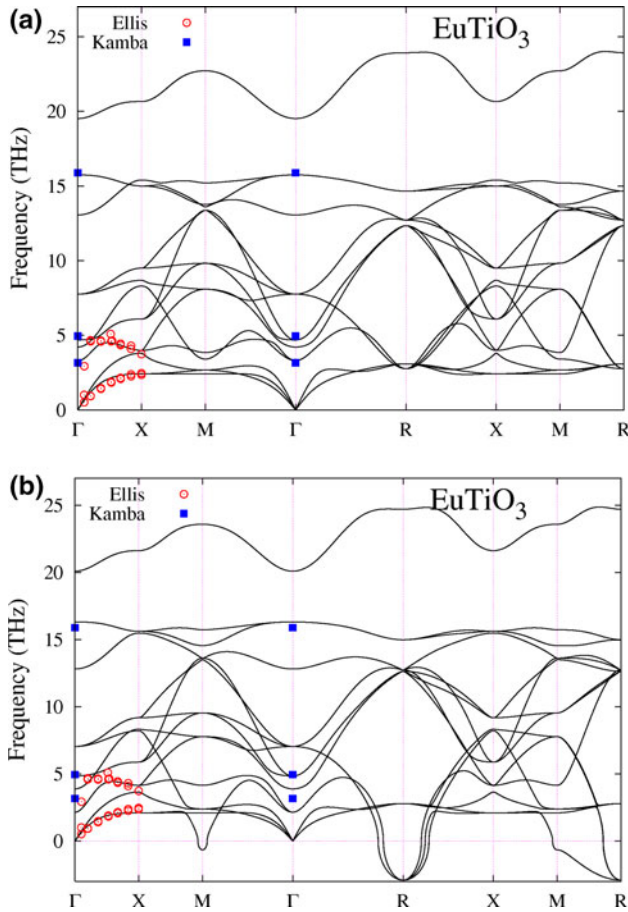


Fig. 3. The calculated phonon dispersions (curves) for cubic EuTiO_3 by the YPHON package using the dynamic short range ordering model (a) and the static displacive model (b) in comparison with inelastic x-ray scattering data²² (circles) and Infrared data²³ (squares) (Color figure online).

FIRST-PRINCIPLES THEORY OF THERMODYNAMICS FOR PHASE WITH THERMAL MIXTURE AMONG MULTIPLE MICROMAGNETIC STATES

For some magnetic systems, such as EuTiO_3 , the energies among different micromagnetic states (i.e., spin configurations) are very close as shown in Fig. 4. In such case the thermal mixing among multiple micromagnetic states at finite temperature T should be considered. We propose that the total partition function of a magnetic system is the summation over the partition functions of individual micromagnetic state as^{5,26,27}

$$Z(N, V, T) = \sum_{\sigma} w^{\sigma} Z(N, \mathbf{V}, T; \sigma) \quad (9)$$

where $Z(N, \mathbf{V}, T; \sigma) = \exp[-NF(\mathbf{V}, T; \sigma)/k_B T]$, N is the number atoms in the considered system, \mathbf{V} the volume, and w^{σ} is the multiplicity of the micromagnetic state σ . It is immediately apparent that $x^{\sigma} = w^{\sigma} Z(N, \mathbf{V}, T; \sigma) / Z(N, V, T)$ is the thermal

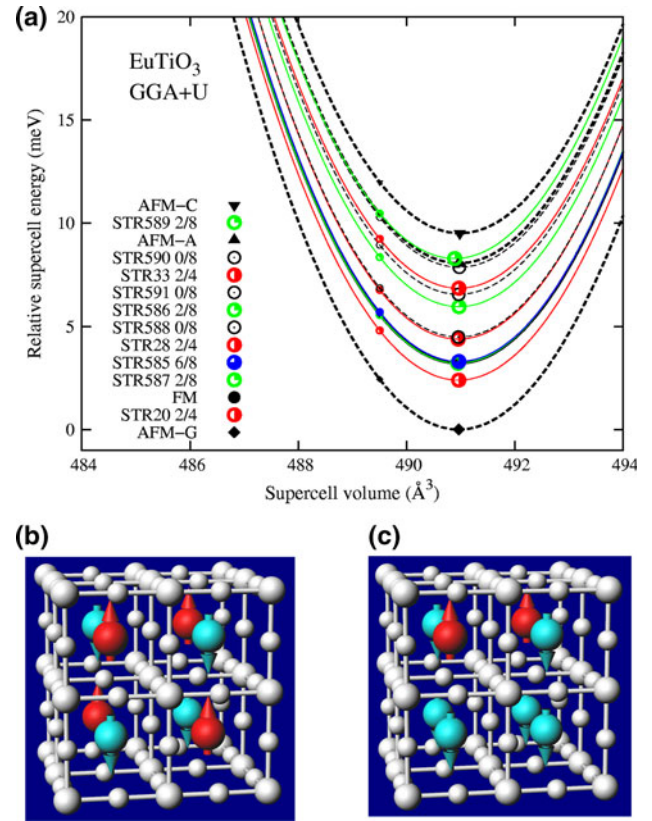


Fig. 4. (a) Energies as a function of volume calculated for all 14 symmetry nonequivalent micromagnetic states obtained from a $2 \times 2 \times 2$ supercell of cubic EuTiO_3 . (b) and (c) show the exemplified spin distributions for the G-type micromagnetic state of EuTiO_3 and a selected micromagnetic state labeled as STR20 of EuTiO_3 , respectively. In (b) and (c), arrows are used to show the spin up/down (red/light-blue) directions at Eu positions. The atomic positions are shown by: Eu, big size (red/light-blue) balls; Ti, medium-size gray balls; O, small-size gray balls (Color figure online).

population of the micromagnetic state σ . Furthermore, with $F = -k_B T \ln Z$, we obtain

$$F(N, V, T) = \sum_{\sigma} x^{\sigma} N F(\mathbf{V}, T; \sigma) + k_B T \sum_{\sigma} x^{\sigma} \ln(x^{\sigma} / w^{\sigma}). \quad (10)$$

Equation 10 relates the total Helmholtz energy of a system with mixing among multiple micromagnetic states $F(N, V, T)$ and the Helmholtz free energy of individual micromagnetic state $F(\mathbf{V}, T; \sigma)$. An important result of Eq. 10 is the configurational entropy due to the mixing among multiple micromagnetic states

$$\Delta S_f(N, V, T) = -k_B \sum_{\sigma} w^{\sigma} [x^{\sigma} / w^{\sigma} \ln(x^{\sigma} / w^{\sigma})] \quad (11)$$

from which the interesting magnetic contribution to the specific heat can be derived as

$$C_m = \frac{1}{k_B T^2} \left\{ \sum_{\sigma} x^{\sigma} (E^{\sigma})^2 - \left[\sum_{\sigma} x^{\sigma} E^{\sigma} \right]^2 \right\} \quad (12)$$

where E^σ indicates the internal energy of the micromagnetic state σ .

Figure 5 shows the ability of the partition function approach on accounting for the excess specific heat for the magnetic phase transition for EuTiO_3 by the bump at ~ 5 K employing the Debye approximation for the calculation of the Helmholtz free energy of the individual micromagnetic state following the procedure of our previous work.⁵

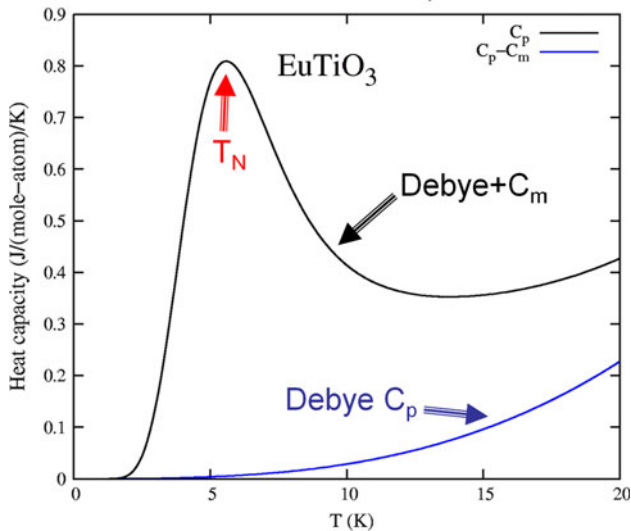


Fig. 5. Total specific heat (C_p , black line) and specific heat due to lattice vibration ($C_p - C_m$, blue line) for EuTiO_3 calculated with the partition function approach (Color figure online).

ESPEI MODELING AUTOMATION

The strength of the CALPHAD method is that data obtained from calculations with CALPHAD descriptions are self-consistent and that these descriptions can be used to extrapolate to multi-component systems, thus making the CALPHAD method attractive for the prediction of properties of complex systems. However, the CALPHAD method also poses a challenge because any modification of a constitutive subsystem has a snowball effect on the description of a multicomponent system in that it affects every description of systems that includes this subsystem, e.g., a change in the binary A-B system affects the description of ternary systems A-B-C, A-B-D, and so on, and it makes reassessments of higher component subsystems necessary. To the best of our knowledge, the thermodynamic databases of experimental data and the automation of database development has been absent. To address this issue, we have been developing a software package named ESPEI (extensible, self-optimizing phase equilibrium computer program),²⁸ which establishes a data infrastructure for storing input data used in thermodynamic modeling and output data for thermodynamic analysis. It has an automation procedure developed to model Gibbs energy functions of individual phases in binary and ternary systems. It relies on extensive thermochemical data from first-principles calculations and was designed mainly by means of Microsoft C# and Structured Query Language (SQL). The GUI of ESPEI for Microsoft Windows is demonstrated in Fig. 6. The proposed next version, ESPEI 2, will be made free

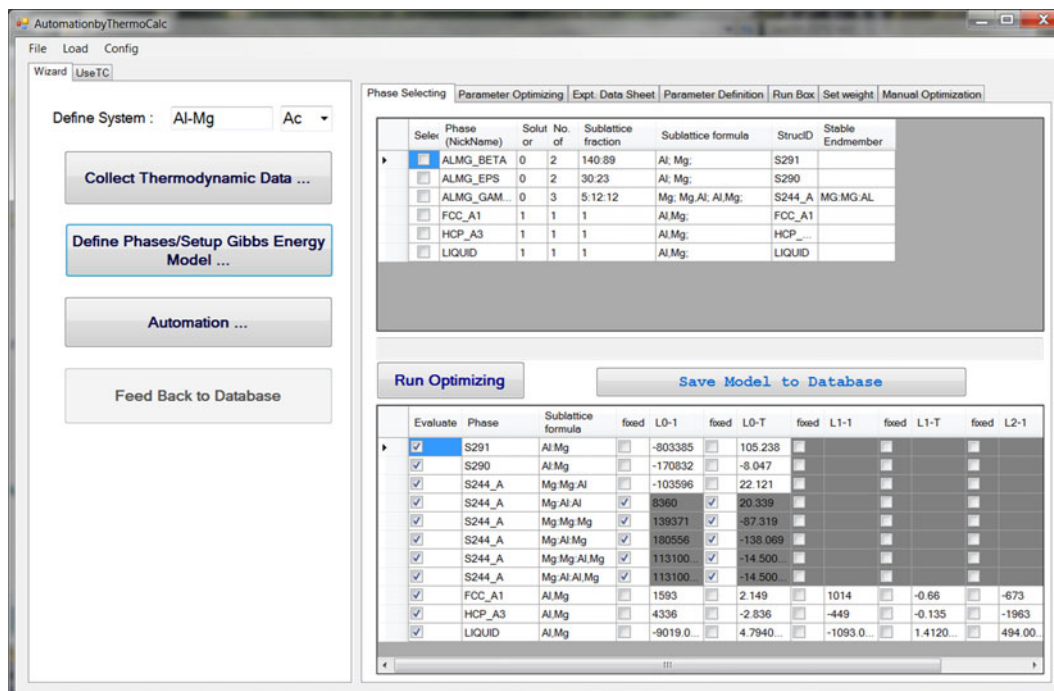


Fig. 6. GUI for ESPEI exemplified with the automatic calculation of phase diagram for the Al-Mg system (Color figure online).

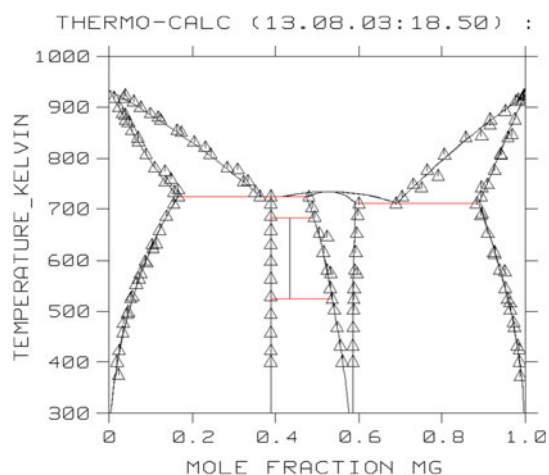


Fig. 7. Phase diagram for the Al-Mg system automatically calculated by ESPEI (Color figure online).

as an open source product for CALPHAD modeling and simulation; it will be available to the community over the World Wide Web.

The overall infrastructure of ESPEI is made of three parts: (I) the GUI in the client side, (II) the databases stored in the server side, and (III) the database development tools in connection with the third party codes, such as Thermo-Calc (Thermo-Calc Software, Stockholm, Sweden). While the databases are stored and managed by Microsoft SQL, the GUI and the communications between different parts are designed by the Microsoft C#. Figure 7 is the phase diagram for the Al-Mg system obtained by means of the automatic calculation of ESPEI through clicking the buttons in the order of “Collect ...”, “Define ...”, and “Automation ...”.

CONCLUSIONS

In conclusion, we have presented the selected results concerning the density functional theory-based alloy thermodynamics. Our works include both the development of fundamental theories on the mixed-space approach to phonons of polar materials, partition function approach to the magnetic phase transition, computerization of the theories, together with the automatic calculation of phase diagram through integrating first-principles calculations and the CALPHAD approach.

ACKNOWLEDGEMENTS

This work was supported by the U.S. Department of Energy, Office of Basic Energy Sciences, Division of Materials Sciences and Engineering under Award DE-FG02-07ER46417 (to Y.W. and L.Q.C.) and by the National Science Foundation (NSF) through Grant No. CHE-1230924 (to Y.W., S.L.S., and Z.K.L.). First-principles calculations were conducted at the National Energy Research Scientific Computing Center, which is supported by the Office of Science of the U.S. Department of Energy under

Contract No. DE-AC02-05CH11231 and the Penn State LION clusters funded by the NSF through Grant No. OCI-0821527.

REFERENCES

1. Z.K. Liu, *J. Phase Equilib. Diffus.* 30, 517 (2009).
2. Y. Wang, S. Curtarolo, C. Jiang, R. Arroyave, T. Wang, G. Ceder, L.Q. Chen, and Z.K. Liu, *CALPHAD-Comput. Coupling Phase Diagr. Thermochem.* 28, 79 (2004).
3. Y. Wang, Z.K. Liu, and L.Q. Chen, *Acta Mater.* 52, 2665 (2004).
4. Y. Wang, S.L. Shang, Z.K. Liu, and L.Q. Chen, *Phys. Rev. B* 85, 224303 (2012).
5. Y. Wang, S.L. Shang, H. Zhang, L.Q. Chen, and Z.K. Liu, *Philos. Mag. Lett.* 90, 851 (2010).
6. D. Shin, A. van de Walle, Y. Wang, and Z.K. Liu, *Phys. Rev. B* 76, 144204 (2007).
7. Y. Wang, J.J. Wang, H. Zhang, V.R. Manga, S.L. Shang, L.Q. Chen, and Z.K. Liu, *J. Phys.-Condens. Matter* 22, 225404 (2010).
8. Y. Wang, C.L. Zacherl, S.L. Shang, L.Q. Chen, and Z.K. Liu, *J. Phys.-Condens. Matter* 23, 485403 (2011).
9. Y. Wang, J.J. Wang, W.Y. Wang, Z.G. Mei, S.L. Shang, L.Q. Chen, and Z.K. Liu, *J. Phys.-Condens. Matter* 22, 202201 (2010).
10. Z.K. Liu, H. Zhang, S. Ganeshan, Y. Wang, and S.N. Mathaudhu, *Scr. Mater.* 63, 686 (2010).
11. A. van de Walle, P. Tiwary, M. de Jong, D.L. Olmsted, M. Asta, A. Dick, D. Shin, Y. Wang, L.Q. Chen, and Z.K. Liu, *CALPHAD-Comput. Coupling Phase Diagr. Thermochem.* 42, 13 (2013).
12. X. Hui, H.Z. Fang, G.L. Chen, S.L. Shang, Y. Wang, J.Y. Qin, and Z.K. Liu, *Acta Mater.* 57, 376 (2009).
13. Z.G. Mei, Y. Wang, S.L. Shang, and Z.K. Liu, *Inorg. Chem.* 50, 6996 (2011).
14. S.L. Shang, L.G. Hector, S.Q. Shi, Y. Qi, Y. Wang, and Z.K. Liu, *Acta Mater.* 60, 5204 (2012).
15. S.L. Shang, Y. Wang, Z.G. Mei, X.D. Hui, and Z.K. Liu, *J. Mater. Chem.* 22, 1142 (2012).
16. Y. Wang, H.Z. Fang, C.L. Zacherl, Z.G. Mei, S.L. Shang, L.Q. Chen, P.D. Jablonski, and Z.K. Liu, *Surf. Sci.* 606, 1422 (2012).
17. Y. Wang, J.E. Saal, P.P. Wu, J.J. Wang, S.L. Shang, Z.K. Liu, and L.Q. Chen, *Acta Mater.* 59, 4229 (2011).
18. Y. Zhao, K.T.E. Chua, C.K. Gan, J. Zhang, B. Peng, Z. Peng, and Q. Xiong, *Phys. Rev. B* 84, 205330 (2011).
19. J.W.L. Pang, w.J.L. Buyers, A. Chernatynskiy, M.D. Lumsden, B.C. Larson, and S.R. Phillpot, *Phys. Rev. Lett.* 110, 157401 (2013).
20. O. Delaire, M.B. Stone, J. Ma, A. Huq, D. Gout, C. Brown, K.F. Wang, and Z.F. Ren, *Phys. Rev. B* 85, 064405 (2012).
21. E. Borissenko, M. Goffinet, A. Bosak, P. Rovillain, M. Cazayous, D. Colson, P. Ghosez, and M. Krisch, *J. Phys.-Condens. Matter* 25, 102201 (2013).
22. D.S. Ellis, H. Uchiyama, S. Tsutsui, K. Sugimoto, K. Kato, D. Ishikawa, and A.Q.R. Baron, *Phys. Rev. B* 86, 220301 (2012).
23. S. Kamba, D. Nuzhnyy, P. Vanek, M. Savinov, K. Knizek, Z. Shen, E. Santava, K. Maca, M. Sadowski, and J. Petzelt, *Europhys. Lett.* 80, 27002 (2007).
24. K.Z. Rushchanskii, N.A. Spaldin, and M. Lezaic, *Phys. Rev. B* 85, 104109 (2012).
25. Y. Wang, L.A. Zhang, S. Shang, Z.-K. Liu, and L.-Q. Chen, *Phys. Rev. B* 88, 024304 (2013).
26. Y. Wang, L.G. Hector, H. Zhang, S.L. Shang, L.Q. Chen, and Z.K. Liu, *Phys. Rev. B* 78, 104113 (2008).
27. Y. Wang, L.G. Hector, H. Zhang, S.L. Shang, L.Q. Chen, and Z.K. Liu, *J. Phys.-Condens. Matter* 21, 326003 (2009).
28. S.L. Shang, Y. Wang, and Z.K. Liu, *Magnesium Technology 2010*, ed. S.R. Agnew, N.R. Neelameggham, E.A. Nyberg, and W.H. Sillekens (Warrendale, PA: TMS, 2010), pp. 617–622.